Journal of the Association of Arab Universities for Basic and Applied Sciences (2014) **16**, 55–63

University of Bahrain

Journal of the Association of Arab Universities for Basic and Applied Sciences

www.elsevier.com/locate/jaaubas
www.sciencedirect.com

دراسة الفعالية الحفزية لحفازات جديدة لازالة غازات NOx,CH,CO المنطلقة من عوادم السيارات

Y. Walid Bizreh[1], Lubna Al-Hamoud[2,*], Malak AL-Joubeh[3]

[1]Head of Laboratory of Adsorption and Catalysis, Chemistry Department, Faculty of Science, Damascus University, Syria
[2]Laboratory of Adsorption and Catalysis, Chemistry Department, Faculty of Science, Damascus University, Syria
[3]Laboratory of Inorganic Physical Chemistry, Chemistry Department, Faculty of Science-Damascus University, Syria

الملخص:

تمّ تحضير ثلاثة حفازات من اكسيد النحاس المحمل على وسادة من مزيج الزيوليت الطبيعي السوري والاردني، البنتونيت السوري و Al_2O_3–CuO. وللمحاكاة الحقلية لحالة محرك السيارة، فقد استخدمنا كمية لا بأس بها من الحبيبات الماكروية للحفاز المستخدم، أما المادة المتفاعلة الابتدائية فهي غازات منطلقة من عوادم السيارات(C.E.G). وقد تمّ اجراء التجارب بواسطة تفاعل ميكروئي شبه نبضي تدفقي باستخدام الغازات المنبعثة من عادم السيارة. عند تطبيق المحفز (Z_JB–CuO, Al_2O_3–CuO) ، فان اقصى نسبة ازالة لـــ CO قدرت بـــ 60% عند الدرجة 250°C ووصلت ازالة CH عند الـــدرجة 400°C الى90%، ولكن بالنسبة للحفاز(ZB–CuO,Al_2O_3–MoO_3–CuO) فلقد بلغت نسبة ازالة CH 80% عند درجة حرارة 360°C ووصلت نسبة ازالة CO الى 78% عند الدرجة نفسها من الحرارة. وقد جعلت البيانات الحفزية من الممكن اقتراح ميكانيكية لكل من التفاعلين الحاصلين. بالنسبة للحفاز(ZB–CuO,Al_2O_3–CuO) تم الوصول الى اعلى نسبة لازالة CH عند درجة الحرارة 450°C. كما تمّ اجراء قياسات امتزاز- لامتزاز النتروجين عند الـــدرجـــة 196°C- وكما تم ايضا دراسة التحليل الحراري وحيود الاشعة السينية لجميع الحفازات المدروسة. اضافة لذلك فقد اجريت مقارنة بين الحفاز التجاري ذو بنية مشط النحل المستخدم في محركات الغازولين والحفازين:(ZB–CuO,Al_2O_3–CuO) و(Z_JB–CuO, Al_2O_3–CuO)

Journal of the Association of Arab Universities for Basic and Applied Sciences (2014) **16**, 55–63

University of Bahrain

Journal of the Association of Arab Universities for Basic and Applied Sciences

www.elsevier.com/locate/jaaubas
www.sciencedirect.com

ORIGINAL ARTICLE

A study on the catalytic activity of new catalysts for removal of NO_x, CH and CO emitted from car exhaust

Y. Walid Bizreh [a], Lubna Al-Hamoud [b,*], Malak AL-Joubeh [c]

[a] *Head of Laboratory of Adsorption and Catalysis, Chemistry Department, Faculty of Science, Damascus University, Syria*
[b] *Laboratory of Adsorption and Catalysis, Chemistry Department, Faculty of Science, Damascus University, Syria*
[c] *Laboratory of Inorganic Physical Chemistry, Chemistry Department, Faculty of Science-Damascus University, Syria*

Received 24 May 2012; revised 6 June 2013; accepted 18 June 2013
Available online 17 July 2013

KEYWORDS

Matrix of mixture from Syrian and Jordanian natural zeolite;
Syrian bentonite and Al2O3–CuO;
ZB–CuO, Al2O3–CuO;
ZJB–CuO, Al2O3–CuO;
ZB–CuO, Al2O3–MoO3–CuO catalysts for de-NO_x;
de-CH and de-CO

Abstract Three catalysts were prepared from copper oxide carried on a matrix of a mixture of Syrian, Jordanian natural zeolite, Syrian bentonite, and Al_2O_3–CuO. As a simulation to the field motor car condition, a good quantity of macrosize granules of the catalyst was used, and the initial reacting agents were the car exhaust gases (C.E.G.). Catalytic experiments were conducted by means of a flow micro pulse–like reactor using the gases emitted from car exhaust. When the (Z_JB–CuO, Al_2O_3–CuO) catalyst was applied, the maximal de-CO conversion was as estimated as 60% at 250 °C, and 90% for de-CH at 400 °C, whereas the de-CH rate conversion of the (ZB–CuO, Al_2O_3–MoO_3–CuO) catalyst was as much as 80% at 360 °C and 78% for de-CO at 360 °C. The catalytic data made it possible to suggest a mechanism for each of the ongoing reactions. A maximal de-CH, conversion rate on the (ZB–CuO, Al_2O_3–CuO) catalyst was reached at 450 °C. The N_2 adsorption–desorption measurements were carried out at (−196 °C), thermal analysis, and X-ray diffraction for the catalysts were studied as well. A comparative study was conducted between the catalysts [(ZB–CuO, Al_2O_3–MoO_3–CuO), and (Z_JB–CuO, Al_2O_3–CuO)] and a honeycomb structure commercial catalyst manufactured for use in gasoline vehicles.

1. Introduction

Selective catalytic reduction of NO_x has attracted considerable interest as a method to control emission from car exhaust. Numerous works have been carried out in this area of research. Copper has been proved to be one of the best metal cations for lean-NO_x catalysts with the optimum level of exchange at 29–42% (Subbiah et al., 2003).The optimized fresh Cu/SUZ–4 catalyst achieved 70–80% of NO/NO_x conversion activity over a wide range of temperatures from 350 °C to 600 °C with the maximum conversion temperature at 450 °C (Subbiah et al., 2003). The catalyst Cu–Al_2O_3 was studied by using linear and branched alkanes with different carbon numbers (Shibata et al., 2002), they found out that the structure of the hydrocarbon had no influence on the selectivity. The Cu–

* Corresponding author. Tel.: +963 991138128.
E-mail addresses: lubna.alhamoud@Gmail.com (L. Al-Hamoud), dr_malak.joubbeh@yahoo.com (M. AL-Joubeh).
Peer review under responsibility of University of Bahrain.

1815-3852 © 2013 Production and hosting by Elsevier B.V. on behalf of University of Bahrain.
http://dx.doi.org/10.1016/j.jaubas.2013.06.001

Mn oxide catalysts were investigated and a reversible deactivation due to the presence of water vapor and SO_2 was observed (Kang et al., 2006). In addition, Takami et al., (1997) have shown that the Pt–Ir–Rh/MFI zeolite catalyst had a higher performance and durability than the current Pt–Rh supported on alumina and ceria catalysts. It was observed that Ag–Al_2O_3 had higher NO conversion to N_2 and selectivity than alumina–supported Pt and Cu–ZSM-5 catalysts for the selective reduction of NO by *n*-octane and *i*-octane (Schimizu et al., 2000). Kuznetsovaa et al. (1993) have found out that the activity of alumochromium oxide catalysts toward hydrocarbons complete oxidation is determined by Cr (VI) cations. Varghese and Wolf (1979) observed that α-alumina – supported Cr exhibited specific activity that was higher than that of bulk Cr_2O_3 and far superior to that of γ-alumina – supported forms. Objective of this work is to prepare a new catalyst from copper oxide supported on matrixes from Jordanian natural zeolite, Syrian bentonite and alumina supported copper oxide and to measure surface properties and catalytic activity for de-CH, de-CO and de-NO_x conversions.

2. Experimental

2.1. Materials

(ZB CuO–Al_2O_3–CuO), (Z_JB–CuO, Al_2O_3–CuO), and (ZB–CuO, Al_2O_3–MoO_3–CuO) were prepared starting from copper oxide carried on a matrix of Jordanian and Syrian natural zeolite, and Syrian bentonite and alumina supported copper oxide. A mass of 66.7 g. of copper nitrate was dissolved in 88.3 ml of hot distillated water (solution I). Solution (I) was impregnated in 166.78 g. of alumina to form a paste, about 50 ml of distillated water was added and mixed with the paste, the paste was put to dry in the shade. The dried product was heated at 110 °C for 4 h. The resulting mass was heated at 550 °C in the oven for 5 h. Next impregnation of Syrian bentonite (B), Syrian zeolite (Z) and Jordanian zeolite (Z_J) with copper nitrate solution was accomplished as follows: 800 g. of Syrian bentonite (B) was impregnated with 800 ml of 0.075 N copper nitrate solution; on the another side, 333 g.

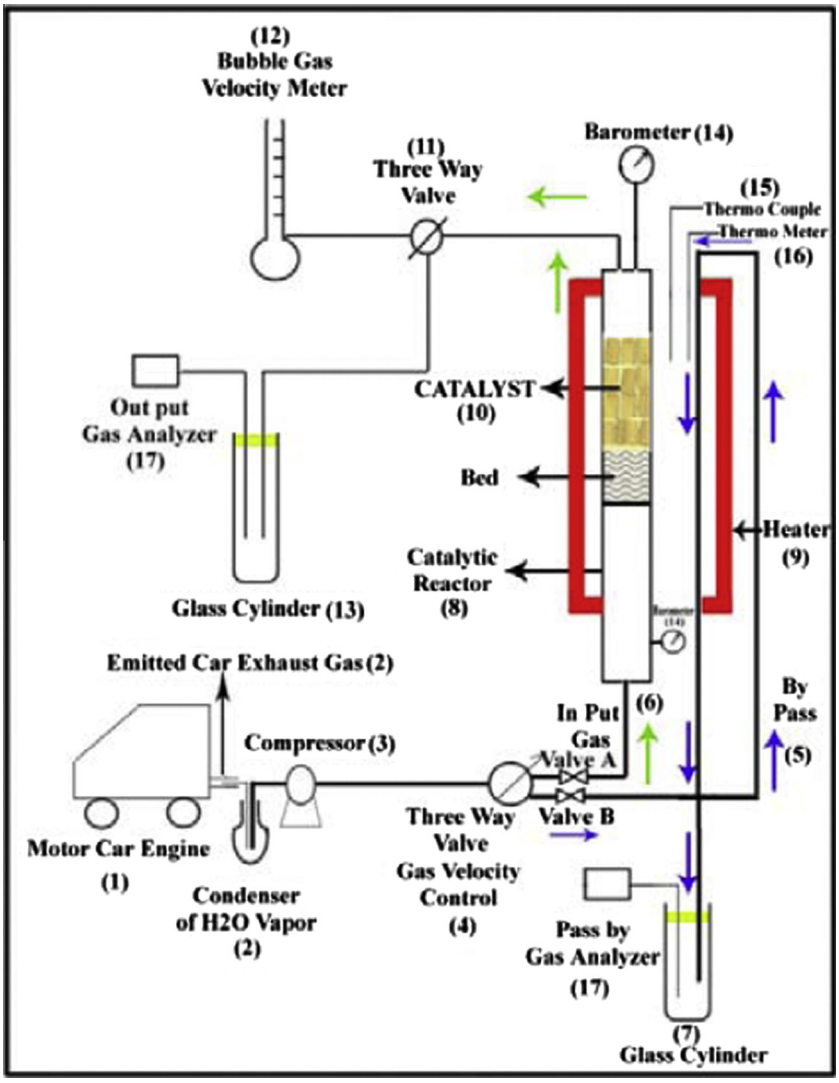

Figure 1 Schematic figure of the reactor system.

of natural Syrian (Z) or Jordanian zeolite (Z_J) was impregnated with 111 ml of 0.6 N copper nitrate solution, and finally, the produced powder of the copper oxide component was divided into two parts, each of them was added to the masses (B), (Z) and (Z_J) respectively. The paste was formed into cylinders of 5 cm in length and external diameter of 4 mm and internal diameter of 2 mm. The received tubes were dried at room temperature in the shade for 7 days. The dried tubes were heated in the Carbolite oven at 550 °C for 5 h. The prepared catalyst was used after cooling in the same oven till the next day. The three catalysts were prepared following the same steps, but to one of the prepared catalysts 6.66 g. of ammonium molybdate was dissolved in 88.3 ml of hot distillated water, and added to a solution similar to solution (I). In order to prepare the third catalyst 66.7 g. of copper nitrate was added and dissolved to the solution (solution I) and the steps mentioned above were followed to receive the catalyst (ZB–CuO, Al_2O_3–MoO_3–CuO).

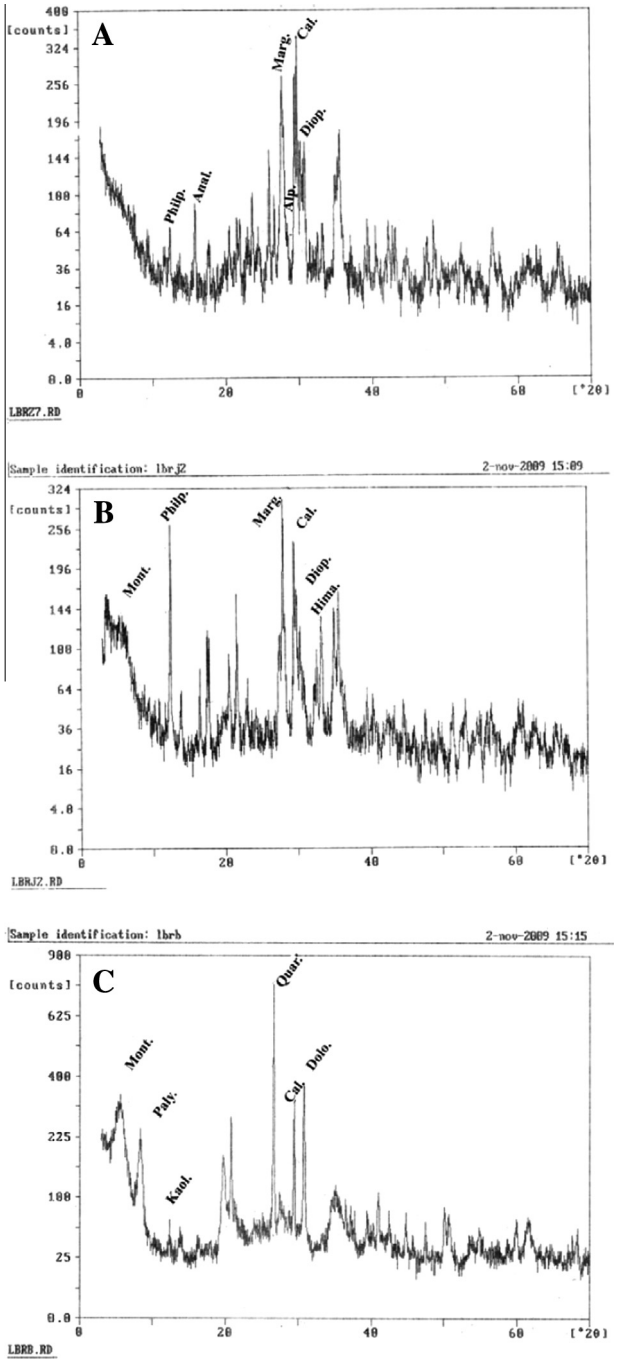

Figure 2 (A) XRD analysis of the Syrian natural zeolite. (B) XRD analysis of the Jordanian natural zeolite. (C) XRD analysis of the Syrian natural bentonite.

2.2. Apparatus and techniques

1. The X–ray fluorescence (XRF) of the catalysts was measured with a Sequential ARL 8410.
2. The X–ray diffraction (XRD) of the catalysts was measured with a Philips PW 1830.
3. The differential thermal analysis has been conducted with Shimadzu DTA & DTG-60H instrument.
4. The surface areas of the catalysts were measured by means of Micromeritics Gemini 3 device using N_2 gases at (−196 °C).
5. Gas analyzer (Kane) for car exhaust emissions.
6. A new developed micro pulse – like flow catalytic pilot plant for catalytic tests.

2.3. Catalytic tests (reactor system)

In order to simulate the motor car condition, the catalytic experiments were conducted by means of a flow micro pulse-like reactor using the gas emitted from car exhaust Fig. 1. A mass of 100 g. of the catalyst (10) was inserted into the reactor (8). The car exhaust gas was transmitted from the vehicle (1) via rubber tubes (2) and a water vapor condenser (2) to a gas compressor (3). The reacting gas passes from the compressor (3) to a three way gas velocity controlling valve (4).

In order to start the measurements, valve (B) is closed simultaneously with valve (A) being opened to make the car exhaust gas pass through to the catalytic reactor (8) heated

Table 1 Results of Structural chemical analysis of Syrian zeolite and Jordanian zeolite.

W. percentage % Oxide	Zeolite (Z)	Zeolite (Z_J)
SiO_2	42.98	42.73
Al_2O_3	15.43	13.36
Fe_2O_3	11.06	10.33
CaO	11.71	10.06
MgO	**4.13**	**8.45**
Na_2O	0.44	0.19
K_2O	1.06	1.71
TiO_2	2.20	2.21
Mn_2O_3	0.14	0.16
SO_3	< 0.02	< 0.01
P_2O_5	0.77	0.36
Cr_2O_3	0.01	–
Cl^-	0.07	–
L.O.I	8.83	9.45

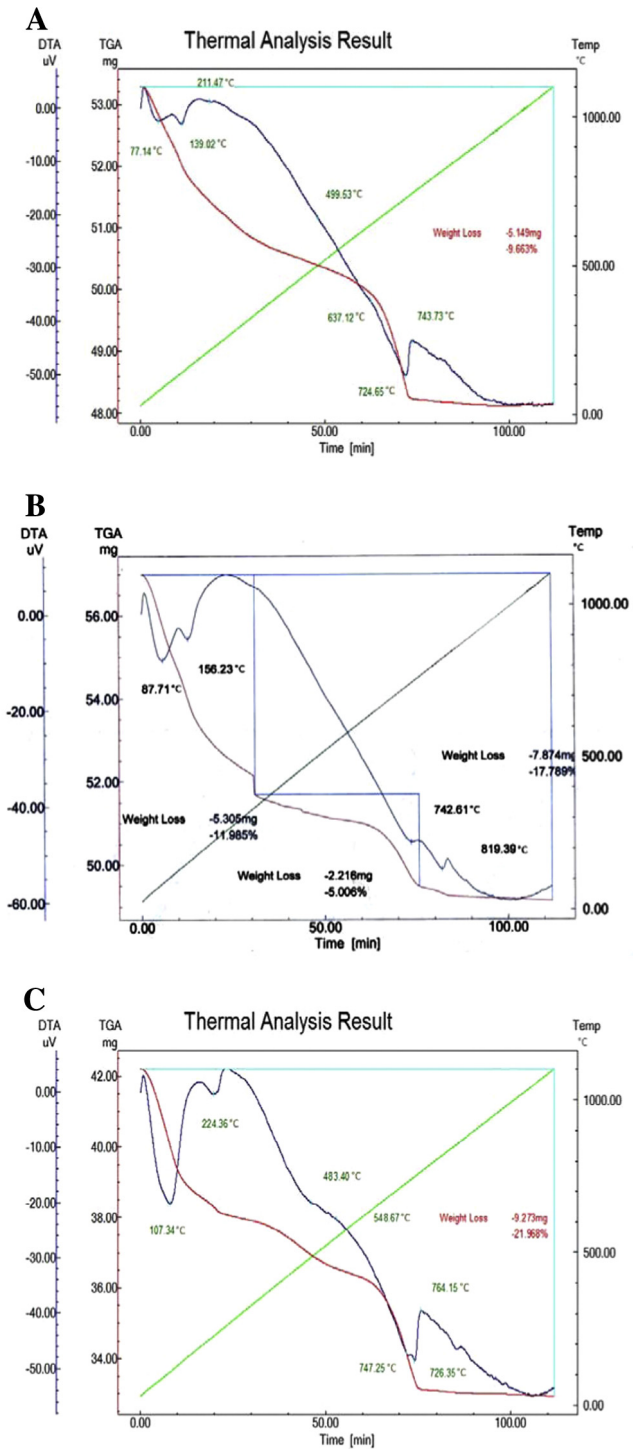

Figure 3 (A) DTA analysis of the Syrian natural zeolite. (B) DTA analysis of the Jordanian natural zeolite. (3C) DTA analysis of the Syrian natural bentonite.

by an oven (9). The reactant with the contact mass gas (10) flows through valve (11) to the bubble gas velocity meter (12) for the output gas. Valve (A) is closed and valve (B) is opened to make the gas flow from valve (B) through tube (5) via heater (9) passing by the catalyst to be analyzed after being collected in a glass cylinder (7), the result of analyses provide the structure of the bypass gas exhaust heated to the same temperature of the heated catalyst in the reactor. The next step is to open valve (A) and shut off the valve (B) at the same moment in order to make a three minute gas pulse pass through the reactor (8) and react with the catalyst layer (10). The resulting gas and products of the catalytic reaction pass trough the three way valve (11) to be collected in the glass cylinder (13) and analyzed by means of the "Kane" gas analyzer (17). Testing the "bypass" gas is to be repeated to make sure that the structure of the initial reacting car exhaust gas before the catalytic measurements is identical to that of the initial gas after measuring the catalytic activity at the same temperature and mean pressure shown in Fig. 1. The inlet mean average composition of the gases emitted from gasoline car exhaust was {(0.15% CO, 13.18% CO_2, 30.83 ppm NO_x, 29.83 ppm NO, 87.17 ppm CH, 4.27% O_2)} ±20%.

3. Results and discussion

3.1. X-ray diffraction

The XRD analysis of the Syrian natural zeolite Fig. 2A shows that it consists of calcite, philpsite, analcime, margret, diopside and alpeite, whereas the Jordanian natural zeolite consists of montmorillonite, philpsite, margret, calcite, diopside and hematite Fig. 2B. The Syrian bentonite includes quartz, dolomite, calcite, palegorskite, kaolinite and montmorillonite shown in Fig. 2C.

3.2. X-ray fluorescence

More detailed results for chemical structure of Z and Z_J that were obtained by means of X-Ray fluorescence are listed in Table 1. The results show close rates of metallic oxides, but MgO is an exception because its content in Z_J is twice that of Z.

3.3. Thermal analysis

DTA analysis of the Syrian zeolite indicates endo-thermal actions at 77.14, 139.02, 724.65 °C, exo-thermal action at 743.73 °C and 9.663% weight loss Fig. 3A, On the other side the Jordanian natural zeolite shows endo-thermal action at 87.71, 156.23 °C, exo-thermal action at 819.39 °C and 17.789% weight loss Fig. 3B. DTA analysis of Syrian bentonite demonstrates endo-thermal actions at 107.34, 224.36, 747.25 °C, exo-thermal action at 764.15 °C, and 21.968% weight loss Fig. 3C. The DTA diagrams for both zeolites show endothermic effect at low temperatures related to the removal of physically bonded water; whereas the endothermic effect of chemically bonded (structural) water removal is observed at higher temperatures and may be followed by phase conversion, the exothermic picks on the diagram are caused by chemical conversions. The wider area of the Z_J endothermic pick, if compared with those for Z zeolite, pick Fig. 3B may be attributed to the montmorillonite present in Z_J.

3.4. Nitrogen adsorption

The surface parameters of the catalysts were measured by means of Micromeritics Gemini 3 device Table 2. The data

Table 2 Data surface properties for the catalysts.

Catalyst	ZB–CuO, Al_2O_3–CuO	ZB–CuO, Al_2O_3–MoO_3–CuO	Z_JB–CuO, Al_2O_3–CuO
Surface area (m^2/gr. BET)	50.4369	52.3407	55.4125
Surface area (m^2/gr. Langmure)	79.1988	81.6539	86.9505
Micropore area m^2/gr.	4.7114	9.2367	5.7339
External surface area m^2/gr.	45.7255	43.1040	49.6786
Micropore value cm^3/gr.	0.0022	0.0005	0.0027
Overall micropore area a certain value P/P_0 cm^3/gr.	0.0673	0.0667	0.0721
Average pore diameter A^0	53.3370	50.9765	52.0421

show a slightly increased surface area for the (Z_JB–CuO, Al_2O_3–CuO) catalyst in comparison with the other two catalysts. Close values are received of the average pore diameter of the catalysts. Introducing MoO_3 to the catalyst (ZB–CuO, Al_2O_3–MoO_3–CuO) has given rise to an increase to its micropore area Table 2.

3.5. Catalytic activity tests

3.5.1. Dependence of conversion rate on time at different temperatures and space velocities

The dependence of NO, NO_x, CH and CO conversions rates on time at different temperatures and space velocities [GHSV = volume flux of exhaust gas per hour/real volume of catalyst (Landong et al., 2005)] was studied for all catalysts, results are represented in Figs. 4 and 5 and Tables 3–5; by means of those tables the (de-CO),(de-CO, de-CH) and (de-NO_x, de-CH) findings for the catalysts will be discussed in the following sections respectively.

3.5.1.1. The de-CO conversion on the(Z_JB–CuO,Al_2O_3–CuO) catalyst. Fig. 4; shows curves for de-CO conversion rates:at a temperature of 250 °C, the maximal de-CO conversion is almost independent of space velocity: (59% at low space velocity and 58% at high space velocity). A little dependence on space velocity was observed at the range of 250–300 °C for the same catalyst: at temperature 300 °C and space velocity range (210.8223–442.5500 h^{-1}), the maximal de-CO conversion at low space velocity is 63% and 58% at high space velocity Fig. 5. The (Z_JB–CuO,Al_2O_3–CuO) catalyst has shown a unique catalytic activity for the de-CO conversion at 250–300 °C and at various space velocities, this may be attributed to the montmorillonite, MgO mentioned above components in the Z_JB–CuO, Al_2O_3–CuO Table 1, and to the possible

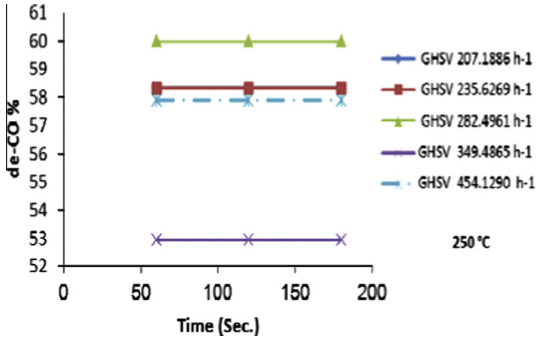

Figure 4 The dependence of CO conversions rate on time at 250 °C for the Z_JB–CuO and Al_2O_3–CuO catalysts.

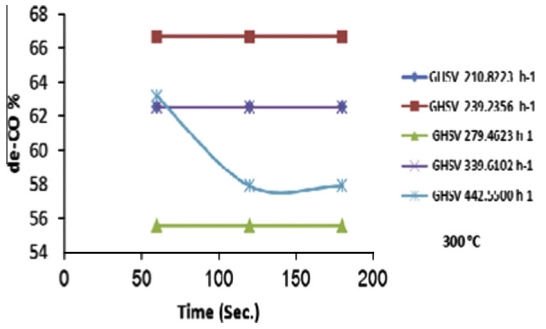

Figure 5 The dependence of CO conversions rate on time at 300 °C for the Z_JB–CuO and Al_2O_3–CuO catalysts.

polarizing power q/r of Mg in MgO. The modified with MoO_3 (ZB–CuO, Al_2O_3–MoO_3–CuO) catalyst was observed to be not active at 250–300 °C.

At a temperature of 360 °C for the (ZB–CuO, Al_2O_3–MoO_3–CuO) catalyst and space velocity range (207.4636–446.3430 h^{-1}): the maximal de-CO conversions at low space velocity were 70% and 60% at high space velocity, the performance of (ZB–CuO, Al_2O_3–MoO_3–CuO) catalyst preceeded that at 350 °C, after being modified with MoO_3. The promoting role of MoO_3 may be due to its *n*-semiconductivity and to the improved surface properties shown in Table 2 caused by adding MoO_3 to the (ZB–CuO, Al_2O_3–CuO) catalyst. The CO molecule may be bonded with MoO_3 because of CO electronic structure [$\sigma_s^2\sigma_s^{*2}(\pi_{xy})^4\sigma_z^2$]. Krilov suggested the following mechanism for (CO) oxidation on metallic oxide catalysts ([Margolis and Ya, 1967] and [Krilov, 1967]):

Obviously, the high catalytic activity of the studied catalysts in terms of de-CO reaction is based on donor–acceptor mechanism because of the low value of the forbidden band gap of copper oxide(1.2 ev) (Krilov, 1967). In addition, the catalytic activity of copper oxide complex catalysts is in accord with the data for the deep oxidation of hydrocarbons received for copper oxide (Krilov, 1967).

3.5.1.2. The (de-CO, de-CH) conversions. occurred simultaneously with the (Z_JB–CuO, Al_2O_3–CuO) catalyst at a temperature of 350 °C and a space velocity range of (216.3712–335.9578 h^{-1}) Table 3: the maximal de-CO and de-CH conversions at low space velocity are 29% and 59%

Table 3 Results for conversion rate of the de-CO and de-CH reactions at 360–350 °C and different space velocities for ZB–CuO, Al_2O_3–MoO_3–CuO and Z_JB–CuO, Al_2O_3–CuO.

Catalysts	Temperature °C	Time (s)	Space Velocity h^{-1}	de-CH%	de-CO%
ZB–CuO, Al_2O_3–MoO_3–CuO	360	180	207.4636	–	70
Z_JB–CuO, Al_2O_3–CuO	350		216.3712	59	29
ZB–CuO, Al_2O_3–MoO_3–CuO	360		251.1583	–	79
Z_JB–CuO, Al_2O_3–CuO	350		251.5614	39	44
ZB–CuO, Al_2O_3–MoO_3–CuO	360		295.8717	–	80
Z_JB–CuO, Al_2O_3–CuO	350		285.5955	31	50
ZB–CuO, Al_2O_3–MoO_3–CuO	360		349.4865	–	75
Z_JB–CuO, Al_2O_3–CuO	350		335.9578	43	29

Table 4 Results for conversion rate of the de-CO and de-CH reactions at 405–400 °C and different space velocities for ZB–CuO, Al_2O_3–MoO_3–CuO and Z_JB–CuO, Al_2O_3–CuO.

Catalysts	Temperature °C	Time (s)	Space velocity h^{-1}	de-CH %	de-CO %
ZB–CuO, Al_2O_3–MoO_3–CuO	405	180	209.9724	71	50
Z_JB–CuO, Al_2O_3–CuO	400		209.1289	92	–
ZB–CuO, Al_2O_3–MoO_3–CuO	405		240.3385	64	40
Z_JB–CuO, Al_2O_3–CuO	400		245.2438	83	–
ZB–CuO, Al_2O_3–MoO_3–CuO	405		278.9655	70	63
Z_JB–CuO, Al_2O_3–CuO	400		288.7605	80	–
ZB–CuO, Al_2O_3–MoO_3–CuO	405		367.5768	32	67
Z_JB–CuO, Al_2O_3–CuO	400		370.4543	60	–

Table 5 Results for conversion rate of the de-NO, de-NO_x and de-CH reactions at 450 °C and different space velocities for ZB–CuO, Al_2O_3–CuO, ZB–CuO, Al_2O_3–MoO_3–CuO and Z_JB–CuO, Al_2O_3–CuO.

Catalysts	Temperature °C	Time (s)	Space velocity h^{-1}	de-CH %	de-NO %	de-NO_x %
ZB–CuO, Al_2O_3–CuO	450	180	252.7830	57	–	–
ZB–CuO, Al_2O_3–MoO_3–CuO			244.0941	61	41	41
Z_JB–CuO, Al_2O_3–CuO			237.7796	92	–	–
ZB–CuO, Al_2O_3–CuO			285.5955	58	–	–
ZB–CuO, Al_2O_3–MoO_3–CuO			294.2001	40	37	40
Z_JB–CuO, Al_2O_3–CuO			285.5955	94	–	–
ZB–CuO, Al_2O_3–CuO			373.7318	50	–	–
ZB–CuO, Al_2O_3–MoO_3–CuO			361.6216	26	28	27
Z_JB–CuO, Al_2O_3–CuO			347.1557	81	–	–
ZB–CuO, Al_2O_3–CuO			466.3298	39	–	–
ZB–CuO, Al_2O_3–MoO_3–CuO			476.2810	20	38	40
Z_JB–CuO, Al_2O_3–CuO			471.9631	60	–	–

respectively; as for high space velocity, de-CO and de-CH conversions were 29% and 43% respectively. As a result, the Z_JB–CuO, Al_2O_3–CuO catalyst is more active than ZB–CuO, Al_2O_3–MoO_3–CuO catalyst for de-CH and de-CO reactions at 350 °C and various space velocities Table 3, this may be attributed to that of the surface area of the catalyst Z_JB–CuO, Al_2O_3–CuO is larger than that of the catalyst ZB–CuO, Al_2O_3–MoO_3–CuO Table 2, in addition, the MgO content mentioned above in the Z_JB–CuO, Al_2O_3–CuO Table 1 may contribute to catalytic activity because of the polarizing effect q/r of Mg in MgO.

The conversion rates for the one way de-CH reaction are listed in Table 4. As shown in this table, the Z_JB–CuO, Al_2O_3–CuO is more active than ZB–CuO, Al_2O_3–MoO_3–CuO at 400 °C and close space velocity and this may be due to the same reasons mentioned in (3.5.1.1). On the other side theZB–CuO, Al_2O_3–MoO_3–CuO is more active than the Z_JB–CuO, Al_2O_3–CuO at 405 °C for de-CH and de-CO reactions two way conversions and this may be attributed to the active sites generated with the rise of temperature.

As to the catalytic de-CH, the related mechanism may be expressed by the deepened oxidation of C_xH_y:

$$C_xH_y + zO_{Ads} \rightarrow (C_xH_yO_z)_{Ads\ Intermediate} \rightarrow mCO_2 + nH_2O$$

which is based on the results of single experiments, that is, the fact of the absence of any reaction in the bypass of the same car exhaust gas flowing through tube (6) in the oven at identical temperatures and flow rates Fig. 1.

3.5.1.3. As for the (de-NOx, de-CH) conversions. the impact of temperature on the activity of (ZB–CuO, Al_2O_3–MoO_3–CuO) catalyst appears clearly at 450 °C as listed in Table 5 when the dual action of n- and p-semiconductors at this relatively high

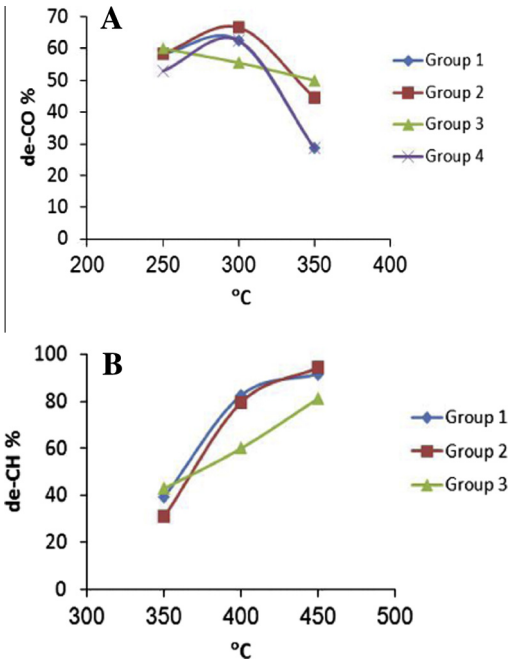

Figure 6 (A) Dependence of the de-CO reaction on temperatures at mean space velocities (groups 1–4) for the (Z_JB–CuO, Al_2O_3–CuO) catalyst. (B) Dependence of the de-CH reaction on temperatures at mean space velocities (groups 1–3) for the (Z_JB–CuO, Al_2O_3–CuO) catalyst.

temperature resulted in sites for de-NO_x in addition to sites for de-CH reactions. Bronsted and Lewis acid sites of zeolite and bentonite surfaces play a role in the de-CH reaction at such temperatures noting that (Z_JB–CuO, Al_2O_3–CuO) catalyst performance is better than (ZB–CuO, Al_2O_3–MoO_3–CuO), those results are in accord with other works [(Zeng Ma et al., 2000; Shibata et al., 2002; Chmielarz et al., 2002; Subbiah et al., 2003; Kubacka et al., 2005)].

The occurrence of de-NO_x catalytic activity at 450 °C may belong to the MoO_3 present in (ZB–CuO, Al_2O_3–MoO_3–CuO) catalyst. The suggested mechanism of the catalytic de-NO, de-NO_x reactions may be interpreted in (Winter, 1971; Amirnazmi et al., 1973; Konsolakis et al., 2001; Ferraris et al., 2002; Balint et al., 2002; Burch et al., 2002) as follows:

$$*_{as} + NO \rightarrow NO_{Ads}$$

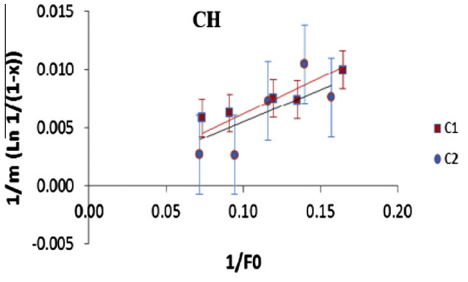

Figure 7 $1/m$ [ln $(1/(1-X))$] as a function of $1/F_0$ for de-CH catalytic reaction for C1 (ZB–CuO, Al_2O_3–CuO) and C2 (ZB–CuO, Al_2O_3–MoO_3–CuO) catalysts at 450 °C.

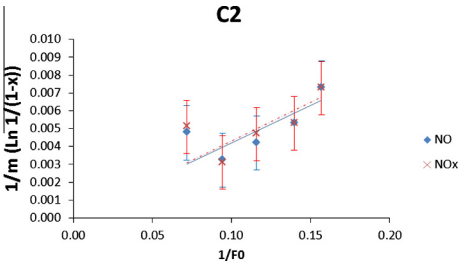

Figure 8 $1/m$ [ln $(1/(1-X))$] as a function of $1/F_0$ for de-NO and de-NO_x catalytic reaction for C2 (ZB–CuO, Al_2O_3–MoO_3–CuO) catalyst at 450 °C.

$$NO_{Ads} + NO_g \rightarrow N_2O + O_{Ads}$$

$$2\,NO_{Ads} \rightarrow N_2 + 2O_{Ads}$$

$$2\,O_{Ads} \rightarrow O_{2g} + 2^*_{as}$$

3.5.2. The dependence of de-CH, de-CO and de-NO_x reactions on temperature at close space velocities may be interpreted as follows

As to the (ZB–CuO, Al_2O_3–CuO) catalyst: first, the maximum for de-CH was reached at 450 °C for a gas mean average composition mentioned in (Section 2.3). Second, the maximum de-NO, de-NO_x was observed at 450 °C. Third, the maximum for de-CH and de-CO conversions was seen at 405 °C and at 360 °C, respectively for "the (ZB–CuO, Al_2O_3–MoO_3–CuO) catalyst, however, a decrease of the de-CO catalytic activity was observed at 450 °C". The presence of molybdenum in the (ZB–CuO, Al_2O_3–MoO_3–CuO) catalyst gave rise to inducing catalytic activity as to de-NO, de-NO_x reactions with a maximum of 52% conversion at 450 °C.

As far as the (Z_JB–CuO, Al_2O_3–CuO) catalyst is concerned, a maximum for de-CO conversion at 250 °C and at 300 °C is shown in Fig. 6A, respectively; besides, a decrease of de-CO catalytic conversion in the range of 350–450 °C was observed. In addition, a maximum of de-CH, conversion is observed at 450 °C. [Results are shown in Figs. 6A and 4B for the given gas mean average composition of the initial gasoline car exhaust gas (C.E.G.): groups 1–4 in Fig. 6A indicate the mean space velocities (211.4607, 242.1413, 282.5180 and 341.6848 h^{-1}, respectively); and groups 1–3 in Fig. 6B indicate the mean space velocities (244.8616, 286.6505 and 351.1893 h^{-1}, respectively)].

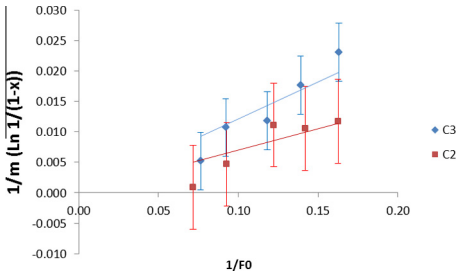

Figure 9 $1/m$ [ln $(1/(1-X))$] as a function of $1/F_0$ for de-CH catalytic reaction for C2 (ZB–CuO, Al_2O_3–MoO_3–CuO) catalyst at 405 °C and C3 (Z_JB–CuO, Al_2O_3–CuO) catalysts at 400 °C.

Table 6 Values of K_Ak by means of the kinetic equation for C1 (ZB–CuO, Al_2O_3–CuO), C2 (ZB–CuO, Al_2O_3–MoO_3–CuO) and C3 (Z_JB–CuO, Al_2O_3–CuO) catalysts.

Temperatures °C	C1	C2	C3
	K_Ak m mol/g sec atm CH	CH	CH
450	0.0027	0.0025	0.0081
405	–	0.0031	–
400	–	–	0.0054
350	–	–	0.0021

3.6. Kinetics and mechanism

The dependence of conversion rate on flow rate of car exhaust gas at different temperatures in the parameters of equation for micro flow reactor was studied. The related kinetic equation used by Bassed and Habgood (1960) is:

$$\frac{1}{m}\ln\frac{1}{1-x} = (273RkK_A)\frac{1}{F_0} \quad (1)$$

where: m: is the mass of the catalyst, x: conversion rate for the de-CH, de-NO_x reaction, K_A: the adsorption equilibrium constant, k: the real rate constant as for the de-NO and de-NO_x reactions, R: general constant gas, F_0: flow rate (F) in an experiment is measured at room temperature and mean pressure and corrected to 0 °C. The results are shown in Fig. 7, those results do not show full agreement with Eq. (1) demonstrating approximately a pseudo first order reaction as to de-CH conversion at 450 °C likely for all the studied catalysts. Besides, the results show agreement with Eq. (1) demonstrating a pseudo first order reaction as to de-NO_x, de-NO at 450 °C for the catalyst (ZB–CuO, Al_2O_3–MoO_3–CuO). Similar results have been received for the (Z_JB–CuO, Al_2O_3–CuO) catalyst in the range of 350–400 °C Figs. 8 and 9. Those results are generally in accord with the results obtained by using another method, where a fractional order for de-NO conversion was observed for a catalyst different from the catalysts used in this work (Serra et al., 2008). The satisfaction of first order equation, however, depends on the nature of the used catalyst, the components of the car exhaust gases, and reaction temperature.

The values of K_Ak calculated by means of the Eq. (1) are listed in Table 6.

Obviously, the high catalytic activity of our catalysts is based on donor–acceptor mechanism because of the low value of the forbidden band gap of copper oxide (1.2 ev). In addition, the catalytic activity of copper oxide complex catalysts is in accord with the data for the deep oxidation of hydrocarbons received for copper oxide (Krilov, 1967).

3.7. Comparison with a commercial catalyst

A comparative study was conducted between the catalysts (ZB–CuO, Al_2O_3–MoO_3–CuO), (Z_JB–CuO, Al_2O_3–CuO) and a honey comb structure commercial catalyst manufactured for use in gasoline vehicles. The experimental measurement was carried out with our developed rig in almost close conditions. Results for CH and CO removal catalyzed by our catalysts and a commercial catalyst are listed in Tables 7 and 8.

4. Conclusions

New catalysts have been prepared from matrices of Syrian and Jordanian zeolites and Syrian bentonite for use as supports of copper oxide catalyzing the de-NO_x, de-NO de-CH and de-CO processes. These catalysts are differing from others, by the presence of a matrix of zeolite and bentonite. In addition, a new catalytic micro pulse-like flow pilot plant has been developed for use as a device for measuring the interaction between the car exhaust pollutants NO, NO_x, CH and CO. The simplicity of preparation and the relatively low cost if compared with the commercial catalyst are the features of the catalysts studied. The catalysts yield high conversion rate for CH and CO at low temperatures. The results show that the maximum conversion rate for de-NO_x and de-NO reactions reached 52% at 450 °C for the (ZB–CuO, Al_2O_3–MoO_3–CuO) catalyst. The maximum conversion rate for de-CH reaction has reached 70% at 405 °C for the (ZB–CuO, Al_2O_3–MoO_3–CuO) catalyst.

Table 7 de-CH and de-CO reaction rates of commercial catalyst compared with the (ZB–CuO, Al_2O_3–MoO_3–CuO) catalyst.

Commercial Catalyst				(ZB–CuO, Al_2O_3–MoO_3–CuO)			
Temperature °C	Space velocity h^{-1}	de-CH %	de-CO %	Temperature °C	Space velocity h^{-1}	de-CH %	de-CO %
350	301.0019	44	29	350	295.8717	–	80
350	491.2500	32	16	350	446.3430	–	60
400	339.6102	47	–	400	367.5768	32	67
450	320.1233	40	–	450	294.2001	51	–

Table 8 de-CH and de-CO reaction rates of commercial catalyst compared with the (Z_JB–CuO, Al_2O_3–CuO) catalyst.

Commercial catalyst				(Z_JB–CuO, Al_2O_3–CuO)			
Temperature °C	Space velocity h^{-1}	de-CH %	de-CO %	Temperature °C	Space velocity h^{-1}	de-CH %	de-CO %
350	301.0019	44	29	350	335.9578	43	29
400	339.6102	47	–	400	370.4543	60	–
450	320.1233	40	–	450	347.1557	81	–

As to de-CH reaction the de-CH conversion was 91% at the range of 400–450 °C for the (Z_JB–CuO, Al_2O_3–CuO) catalyst. The maximum conversion rate for de-CO reaction has reached 70% at 360 °C for the (ZB–CuO, Al_2O_3–MoO_3–CuO) catalyst. As to de-CO reaction, conversion rate was about 63% at 300 °C for the (Z_JB–CuO, Al_2O_3–CuO) catalyst. The presence of molybdenum in the (ZB–CuO, Al_2O_3–MoO_3–CuO) catalyst did not affect the catalytic activity for de-CH conversions, however, it resulted in an additional catalytic activity for de-NO_x reaction at 450 °C and de-CO at the range of 360–405 °C; those results may be due to the impact of both n-type (Al_2O_3, MoO_3) and p-type (CuO) semiconductor electron effects. The reaction kinetics was studied; the results make it reasonable to suggest a close to pseudo first order reaction as to de-CH conversion in conditions of experiments for all the catalysts. A comparative study was conducted between the catalysts (ZB–CuO, Al_2O_3–MoO_3–CuO), (Z_JB–CuO, Al_2O_3–CuO) and a honeycomb structure commercial catalyst manufactured for use in gasoline vehicles; the experimental measurements were carried out with the developed rig in almost close conditions, results for the compared catalysts were received.

References

Amirnazmi, A., Benson, J.E., Boudart, M., 1973. Oxygen inhibition in the decomposition of NO on metal oxides and platinum. Journal of Catalysis 30, 55–65.

Balint, I., Miyazaki, A., Aika, K., 2002. NO reduction by CH_4 over well–structured Pt nanocrystals supported on γ–Al_2O_3. Applied Catalyst B 37, 217–229.

Bassed, D.W., Habgood, H.W., 1960. A gas chromatographic study of the catalytic isomerization of cyclopropane. Journal of Physical Chemistry 64, 769–773.

Burch, R., Bareen, J.P., Meunier, F.C., 2002. A review of the selective reduction of NO_x with hydrocarbons under lean–burn conditions with non–zeolite oxide and platinum group metal catalysts. Applied Catalyst B 39 (4), 283–303.

Chmielarz, L., Kustrowski, P., Lasocha, A.R., Majda, D., Dziembaj, R., 2002. Catalytic activity of Co–Mg–Al, Cu–Mg–Al and Cu–Co–Mg–Al mixed oxides derived from hydrotalcites in SCR of NO with ammonia. Applied Catalyst B 35 (3), 195–210.

Ferraris, G., Fierro, G., Jacono, M.L., Inversi, M., Dragone, R., 2002. A study of the catalytic activity of cobalt–zinc manganites for the reduction of NO by hydrocarbons. Applied Catalyst B 36 (4), 251–260.

Kang, M., Park, E.D., Kim, J.M., Yie, J.E., 2006. Cu–Mn mixed oxides for low temperature NO reduction with NH_3. Catalysis Today 111 (3-4), 236–241.

Konsolakis, M., Yentekakis, I.V., Palermo, A., Lambert, R.M., 2001. Optimal promotion by rubidium of CO + NO reaction over Pt/γ–Al_2O_3 catalysts. Applied Catalyst B 33 (4), 293–302.

Krilov, O.V., 1967. Katalys Nemetalami. Chemical Leningrad Branch p. 90, 154.

Kubacka, A., Janas, I., Wloch, E., Sulikowski, B., 2005. Selective catalytic reduction of nitric oxide over zeolite catalysts in the presence of hydrocarbons and the excess of oxygen. Catalysis Today 101, 139–145.

Kuznetsovaa, L.L., Paukshtis, E.A., Shkurinaa, G.P., Shkrabina, R.A., Koryabkina, N.A., Arendarskii, D.A., Barannik, G.B., Ismagilov, Z.R., 1993. Chromium catalysts for hydrocarbons destruction. Catalysis Today 17 (1–2), 209–216.

Landong, L., Jixin, C., Shujuan, Z., Fuxiang, Z., Naijia, G., Tianyou, W., Shuliang, L., 2005. Selective catalytic reduction of nitrogen oxides from exhaust of lean burn engine over in–situ synthesized Cu–ZSM–5 cordierite. Environment Science Technology 39 (8), 2841–2847.

Margolis, L., Ya, 1967. Catalytic oxidation of hydrocarbons. Chemical Leningrad Branch, 121.

Schimizu, K., Satsuma, A., Hattori, T., 2000. Catalytic performance of Ag–Al_2O_3 catalyst for the selective catalytic reduction of NO by higher hydrocarbons. Applied Catalysis B Environmental 25 (4), 239–247.

Serra, R., Vecchietti, M.J., Miro, E., Boix, A., 2008. In, Fe–zeolites: Active and stable catalysts for SCR of NOx–Kinetics, characterization and deactivation studies. Catalysis Today 133–135, 480–486.

Shibata, J., Schimizu, K., Satsuma, A., Hattori, T., 2002. Influence of hydrocarbon structure on selective catalytic reduction of NO by hydrocarbons over Cu–Al_2O_3. Applied Catalysis B Environmental 37 (3), 197–204.

Subbiah, A., Cho, B.K., Blint, R.J., Gujar, A., Price, G.L., Yie, J.E., 2003. NOx reduction over metal–ion exchanged novel zeolite under lean conditions: activity and hydrothermal stability. Applied Catalysis B Environmental 42 (2), 155–178.

Takami, A., Takemoto, T., Lwakuni, H., Yamada, K., Shigetsu, M., Komatsu, K., 1997. Zeolite–supported precious metal catalysts for NOx reduction in lean burn engine exhaust. Catalysis Today 35 (1–2), 75–81.

Varghese, P., Wolf, E.E., 1979. CO oxidation on α–alumina–supported chromia catalysts. Journal of Catalysis 59, 100–108.

Winter, E.R.S., 1971. The catalytic decomposition of nitric oxide by metallic oxides. Journal of Catalysis 22, 158–170.

Zeng Ma, A., Muhler, M., Grunert, W., 2000. Selective catalytic reduction of NO by ammonia over Raney–Ni supported Cu–ZSM–5. II. Interactions between support and supported Cu–ZSM–5. Applied Catalysis B Environmental 27, 37–47.